Classical and quantal studies of the satellite features in the absorption spectra of lithium ($2s$-$2p$) perturbed by helium

K. Alioua[1,2] and M. Bouledroua[1]
[1]*Laboratoire de Physique des Rayonnements, Badji Mokhtar University, B.P. 12, Annaba 23000, Algeria*
[2]*Souk-Ahras University Center, Souk-Ahras 41000, Algeria*
(Received 10 July 2006; published 27 September 2006)

This work reports a theoretical analysis of the Li($2s \rightarrow 2p$) photoabsorption spectra when the lithium atoms are evolving in a ground helium buffer gas. The influence of temperature on the far-line wing spectra is particularly examined by adopting classical and full quantum-mechanical approaches. The computations show the appearance, above approximately 1000 K, of satellite structures in the blue wing around the wavelength 536 nm. The data obtained in the range of temperature 500–3000 K agree very well with those already calculated with different theoretical methods.

DOI: 10.1103/PhysRevA.74.032711 PACS number(s): 32.80.−t, 31.50.Bc, 31.50.Df, 32.70.Jz

I. INTRODUCTION

As already reported by Babb, Kirby, and Chung [1], a new frontier has been opened with the discovery of numerous brown dwarfs and extrasolar giant planets. The observations revealed that the atmospheric environments of these astronomical objects have many similarities and that the atmospheric opacities are primarily from the alkali metals [2–4]. That is the reason why the alkali-metal resonance lines are used in the theoretical calculations and experimental measurements of the spectra as important tools for determining the properties of the brown dwarfs and planet environments in which they are produced. The resonance-line broadening of the alkali metals interacting with like or unlike atoms has been a subject of many theoretical and experimental studies. For example, full descriptions have been accomplished on the pressure broadening of lithium, sodium, and potassium when perturbed by their respective parent gases in Refs. [5–7] and by rare-gas atoms in Refs. [3,4,8–10]. One may also mention here the theoretical works on the self-broadening of hydrogen [11] and helium [12].

To the best of our knowledge, the absorption spectra produced by lithium atoms evolving in a helium bath have not been explored experimentally. However, a few theoretical studies are available [9,13–18], such as the work of Herman and Sando [15], where they have determined the emission spectra using classical and quantum-mechanical methods with the assumption of a constant transition dipole moment (TDM), and the most recent investigation of Zhu *et al.* [9], who have essentially treated the emission spectra of the LiHe system.

In this paper, we present our classical and quantal calculations of the photoabsorption spectra of Li($2s$-$2p$) perturbed by He($1s^2$) atoms. We particularly focus our attention on the study of the blue and red wings of the absorption spectra, analyze their possible satellite structures at various temperatures, and compare the results with previous calculations whenever available.

All the data below are given in atomic units (a.u.) unless otherwise specified.

II. THEORY

The purpose of this work is to study the pressure broadening of the lithium $2s$-$2p$ resonance absorption line in the red and blue wings when the Li atoms are evolving in a bath of He atoms. Such a broadening arises from the binary collisions if the density of the Li+He gas mixture is assumed to be sufficiently low. The shape of the broadened line can be modeled as the absorption of the radiation by the LiHe quasimolecules formed from the temporary association of Li and He atoms. At thermal equilibrium, the Li($2s$) and He($1s^2$) atoms approach each other along the $X\,^2\Sigma^+$ molecular state. During the absorption process, the LiHe quasimolecule can absorb a photon of energy $h\nu$, with h being the Planck's constant and ν the absorption frequency, to make a transition towards one of the molecular states $A\,^2\Pi$ or $B\,^2\Sigma^+$ corresponding to the Li($2p$)+He($1s^2$) interaction. The physical parameter that characterizes the photoabsorption process is typically the absorption coefficient k_ν, which is defined as the photon number absorbed per unit time, per unit volume, per unit frequency interval. We use the atomic density-independent reduced-absorption coefficient $k_r(\nu) = k_\nu/(n_{\mathrm{Li}} n_{\mathrm{He}})$ at frequency ν, with n_{Li} and n_{He} being the lithium and helium atomic densities, respectively. If n_{Li} and n_{He} are in units of cm^{-3}, the coefficient k_r has units of cm^5. Classical and quantal approaches are generally considered to determine the line profile [19–21].

A. Classical approximation

In the frame of the quasistatic approximation, the classical expression for the reduced-absorption coefficient for a given frequency ν that corresponds to a transition from the lower molecular state of potential energy $V''(R)$ to an upper molecular state of potential energy $V'(R)$ is given by [19–21]

$$k_r(\nu) = \frac{8\pi^3 \nu}{3hc} g \sum_R 4\pi R^2 |D(R)|^2 \left| \frac{d(\Delta V)}{dR} \right|^{-1} \exp\left(- \frac{V''(R)}{k_B T} \right). \tag{1}$$

In this equation, c is the velocity of light, k_B is the Boltzmann's constant, T is the absolute temperature, and g is the

degeneracy of the final state. Both lower and upper states are interrelated by the transition dipole moment $D(R)$ at the internuclear separation R. The summation in Eq. (1) is over the so-called Condon points $R=R_c$ corresponding to the same frequency ν. These points are the solutions of the equation

$$\Delta V = V'(R) - V''(R) = h(\nu - \nu_0), \tag{2}$$

where ν_0 is the unperturbed line frequency of the radiating atom. Furthermore, Szudy and Baylis [19,21] have modified the above Eq. (1) by multiplying the expression under the summation by the factor $|36\pi z_c|^{1/2}L(z_c)$ where

$$z_c = \frac{1}{2}\left(\frac{\mu}{k_B T}\right)^{1/3}\left|\frac{1}{\hbar}\frac{d(\Delta V)}{dR}\right|^{2}\left|\frac{1}{\hbar}\frac{d^2(\Delta V)}{dR^2}\right|^{-4/3}, \tag{3}$$

μ is the reduced mass of the two colliding atoms, and $L(z_c)$ is the function given by

$$L(z_c) = \int_0^\infty t^{-2}\mathrm{Ai}(-z_c t)^2 \exp(-t^{-3})dt, \tag{4}$$

where $\mathrm{Ai}(y)$ is the well-known Airy function. As reported in Ref. [19], $L(z_c)$ describes the total line shape in the wings.

B. Absorption quantum theory

Keeping in mind that the interacting atoms considered in this work are not identical, we have used the relationships of the quantal reduced-absorption coefficients $k_r(\nu)$ as formulated by Chung, Kirby, and Babb [7]. Since large values of the rotational quantum numbers J are involved, we may assume $J'' \simeq J' = J$, where J'' and J' are, respectively, the lower and the upper rotational quantum numbers.

The *free-free* (ff) reduced-absorption coefficient $k_r^{ff}(\nu)$ at frequency ν corresponding to the transitions from all the lower continuum levels $(\epsilon'', J'', \Lambda'')$ to all the upper continuum levels $(\epsilon', J', \Lambda')$ is given by

$$k_r^{ff}(\nu) = \frac{8\pi^3\nu}{3c}\omega\left(\frac{2\pi\hbar^2}{\mu k_B T}\right)^{3/2}\int_0^\infty d\epsilon' \sum_J (2J+1) \times |\langle \phi_{\epsilon' J' \Lambda'}|D(R)|\phi_{\epsilon'' J'' \Lambda''}\rangle|^2 e^{-\epsilon''/k_B T}, \tag{5}$$

where Λ'' and Λ' denote the projection of the electronic orbital angular momentum on the internuclear axis for the ground and excited states. The continuum-energy levels ϵ'' and ϵ', respectively, of the initial and final electronic states, are correlated via $\epsilon'' = h(\nu_0 - \nu) + \epsilon'$. The factor ω represents the probability that the interacting atoms form a quasimolecule in the lower electronic state

$$\omega = \frac{2 - \delta_{0,\Lambda'+\Lambda''}}{2 - \delta_{0,\Lambda''}}\frac{(2S_m+1)^2}{(2S_r+1)(2S_p+1)}, \tag{6}$$

where δ is the Kronecker symbol and S_m, S_r, and S_p are the spin multiplicities for the molecule (m), the radiating (r), and the perturbing (p) atoms, respectively.

On the other hand, the *free-bound* (fb) reduced-absorption coefficient $k_r^{fb}(\nu)$ at frequency ν derived for the transition from all the lower continuum levels $(\epsilon'', J'', \Lambda'')$ to a set of bound levels of the upper electronic states (v', J', Λ') is given by

$$k_r^{fb}(\nu) = \frac{8\pi^3\nu}{3c}\omega\left(\frac{2\pi\hbar^2}{\mu k_B T}\right)^{3/2}\sum_{v'J}(2J+1) \times |\langle \phi_{v' J' \Lambda'}|D(R)|\phi_{\epsilon'' J'' \Lambda''}\rangle|^2 e^{-\epsilon''/k_B T}, \tag{7}$$

where v' is the vibrational quantum number.

The matrix elements shown in Eqs. (5) and (7) are determined by using the radial-wave functions $\phi(R)$ of the considered states. Assuming the Born-Oppenheimer approximation, these wave functions are a solution of the radial-wave equation

$$\frac{d^2\phi(R)}{dR^2} + \left[\frac{2\mu E}{\hbar^2} - \frac{2\mu V(R)}{\hbar^2} - \frac{J(J+1)-\Lambda^2}{R^2}\right]\phi(R) = 0. \tag{8}$$

The energy of the relative motion is $E>0$ for the free states associated with the *energy*-normalized wave function $\phi(R) = \phi_{\epsilon J\Lambda}(R)$ and $E<0$ for the bound states associated with the *space*-normalized wave function $\phi(R) = \phi_{vJ\Lambda}(R)$. The rotationless potential $V(R)$ and the energy E are measured with respect to the dissociation limit.

The reduced-absorption coefficients as described in both quantal and classical approaches are sensitive to the interaction potentials of the colliding atoms and depend explicitly on the transition dipole moments $D(R)$.

III. POTENTIALS

To construct the potential-energy curves through which one lithium atom Li$(2s)$ or Li$(2p)$ interacts with He$(1s^2)$, we have chosen the most reliable *ab initio* data points that are available in the literature, which are smoothly connected to the short-range potential $V(R) \sim \alpha \exp(-\beta R)$ and to the long-range potential $V(R) \sim -C_6/R^6 - C_8/R^8 - C_{10}/R^{10}$. The corresponding molecular symmetries are $X\,^2\Sigma^+$ for the ground state and $A\,^2\Pi$ and $B\,^2\Sigma^+$ for the excited state.

To construct the $X\,^2\Sigma^+$ state, we combined some *ab initio* values obtained from Czuchaj *et al.* [22], Staemmler [23], and Jeung [24]. This potential is very shallow and shows a well depth of 6.787×10^{-6} at the position 11.553, which is comparable to 6.790×10^{-6} and 11.560 of Staemmler [23]. For the $A\,^2\Pi$ potential, we adopted the energy values of Jeung [24] modified with those of Behmenburg *et al.* [16]. This potential displays a well depth of 4.55×10^{-3} occurring at 3.395. These data compare well with the experimental values 4.647×10^{-3} and 3.370 of Lee *et al.* [25] and with 4.638×10^{-3} and 3.400 of Nakayama and Yamashita [26]. The $B\,^2\Sigma^+$ molecular state is constructed from the data points of Jeung [24] and Krauss, Maldonado, and Wahl [27]. This potential is mainly repulsive though it presents a well at the position 17.027 with a depth of 1.511×10^{-6}. Jungen and Staemmler [28] found for this state the values 18.0 and 1.367×10^{-6}, respectively. For all the potentials, the adopted values of the constants α and β and of the dispersion coef-

TABLE I. Short- and long-range constant parameters adopted for the constructed ground and excited LiHe potentials.

Molecular states	Short-range		Long-range		
	α	β	C_6	C_8	C_{10}
$X\,^2\Sigma^+$	0.573	1.146	22.507[a]	1083.16[a]	72 606.10[a]
$A\,^2\Pi$	30.721	3.022	28.267[b]		
$B\,^2\Sigma^+$	2.926	1.615	50.686[c]	2816.00[c]	

[a]Reference [29].
[b]Reference [30].
[c]Reference [31].

ficients C_n ($n=6$, 8, or 10) are listed in Table I. Our construction of the potential-energy curves relative to these molecular symmetries is given in Fig. 1. Besides, we have determined the vibrational levels of the X, A, and B molecular states by using, with slight modifications, the FORTRAN package Level 7.4 written by Le Roy [32]. The calculations found no bound levels with the $B\,^2\Sigma^+$ state. For the $X\,^2\Sigma^+$ and $A\,^2\Pi$ states, they show only one bound level for the ground state and seven for the excited state. Both results are confirmed by those obtained by the semiclassical method of Gribakin and Flambaum [33]. Our data are listed in Table II in which we compare the A-state results with the Jungen and Staemmler data [28]. The discrepancies are important with the higher vibrational values.

Quantum mechanically, the allowed transitions are $X \rightarrow B$ and $X \rightarrow A$. The satellite structures are expected to be observed where the extrema of the potential differences, namely, $\Delta V = V_B(R) - V_X(R)$ and $\Delta V = V_A(R) - V_X(R)$, occur. Figure 2 presents these differences. As it can be seen from this figure, a satellite should therefore appear near 536 nm in the blue wing and 1012 nm in the red wing. One may also notice that the short-range potential forms, lying between $R \simeq 2$ and $R \simeq 4$, should strongly influence the position and the shape of the expected satellite peaks.

TABLE II. Rotationless vibrational levels, $-E(v,J=0)$, found for the $X\,^2\Sigma^+$ and $A\,^2\Pi$ molecular symmetries.

v	$X\,^2\Sigma^+$	$A\,^2\Pi$	
		This work	Jungen and Staemmler [28]
0	0.1371×10^{-7}	0.3808×10^{-2}	0.3235×10^{-2}
1		0.2494×10^{-2}	0.2050×10^{-2}
2		0.1485×10^{-2}	0.1148×10^{-2}
3		0.7582×10^{-3}	0.5194×10^{-3}
4		0.2975×10^{-3}	0.1686×10^{-3}
5		0.6329×10^{-4}	0.2278×10^{-4}
6		0.1113×10^{-5}	

IV. TRANSITION DIPOLE MOMENTS

The ground $X\,^2\Sigma^+$ state is connected by dipole moments to the excited $B\,^2\Sigma^+$ and $A\,^2\Pi$ states. We constructed both transition dipole moments, namely, $D_{\Sigma\Sigma}(R)$ and $D_{\Sigma\Pi}(R)$, from the data points provided by Jeung [34]. His TDM data points are listed in Table III. We extended the $\Sigma\Sigma$ data with one value ($R=2$, $D_{\Sigma\Sigma}=1.614$) from Pascale [35]. Figure 3 represents our TDM results and shows the data points we have used.

At large distances R, we adopted the asymptotic form proposed by Chu and Dalgarno [36]

$$D(R) \sim D_0 + \frac{A}{R^3}, \tag{9}$$

where $D_0=+2.351$ is the TDM value to which $D(R)$ converges as $R \rightarrow \infty$. For the $\Sigma\Sigma$ transitions, we used their value $A=+6.536$ given in Ref. [36]. For the $\Sigma\Pi$ transitions, the available data values do not match the long-range form provided in Ref. [36]. We hence fitted the last five points with a form similar to Eq. (9). Our calculations could yield $A=+1.147$. In the short-range interval, i.e., $R<2$, we forced the transition dipole moments to follow a linear form $D(R) \sim a+bR$. The obtained values of a and b are $a=1.170$ and

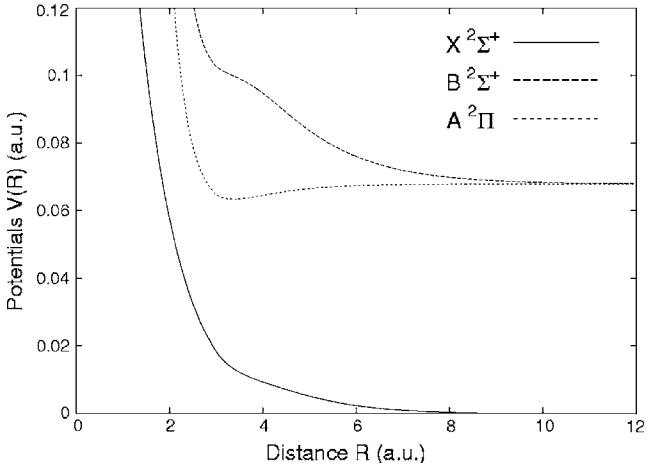

FIG. 1. The constructed ground $X\,^2\Sigma^+$ and excited $A\,^2\Pi$ and $B\,^2\Sigma^+$ LiHe potential-energy curves.

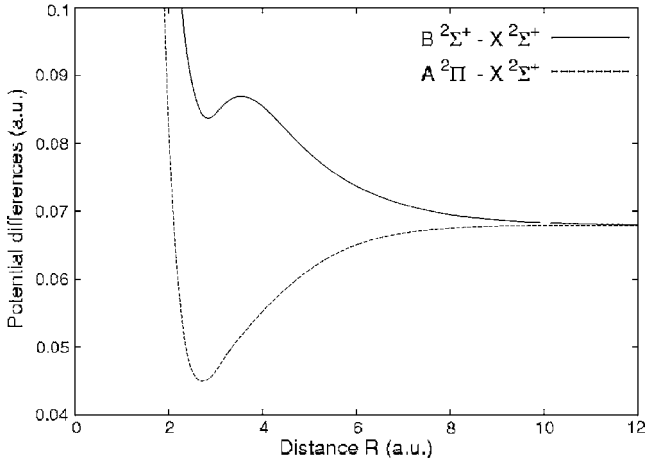

FIG. 2. Potential differences ΔV_{B-X} and ΔV_{A-X} vs the internuclear separation R.

TABLE III. The adopted TDM data points for the construction of $D(R)$ relative to the X-B and X-A transitions. Both data sets are provided by Jeung [24].

Distance R	Data points	
	$X\,^2\Sigma^+$-$B\,^2\Sigma^+$	$X\,^2\Sigma^+$-$A\,^2\Pi$
2.00	1.6140	
2.50		2.3255
2.75		2.3333
3.00	1.7689	2.3415
3.25	1.8303	2.3496
3.50	1.9146	2.3576
3.75	1.9992	2.3643
4.00	2.0666	2.3695
4.25	2.1137	2.3728
4.50	2.1460	2.3744
4.75	2.1695	2.3744
5.00	2.1882	2.3732
5.50	2.2185	2.3690
6.00	2.2444	2.3640
7.00	2.2872	2.3563
8.00	2.3175	2.3530
9.00	2.3361	2.3515
10.0	2.3459	2.3511
11.0	2.3505	
12.0	2.3522	
13.0	2.3527	
14.0	2.3527	
15.0	2.3525	
16.0	2.3523	
17.0	2.3521	
18.0	2.3519	
19.0	2.3518	
20.0	2.3517	
21.0	2.3516	
22.0	2.3515	
24.0	2.3514	
26.0	2.3513	
30.0	2.3512	

$b=0.222$ for the transition $\Sigma\Sigma$ and $a=2.255$ and $b=0.030$ for the transition $\Sigma\Pi$.

V. LIFETIME

Generally, one of the best ways to assess the accuracy of our adopted potentials and transition dipole moments is the determination of the lifetimes of the rotational-vibrational states. We calculated the spontaneous emission transition probabilities and lifetimes of rotational-vibrational levels of the $A\,^2\Pi$. When we neglect the change in the rotational quantum number, namely, $J=J'\simeq J''$, the lifetime τ is then [6]

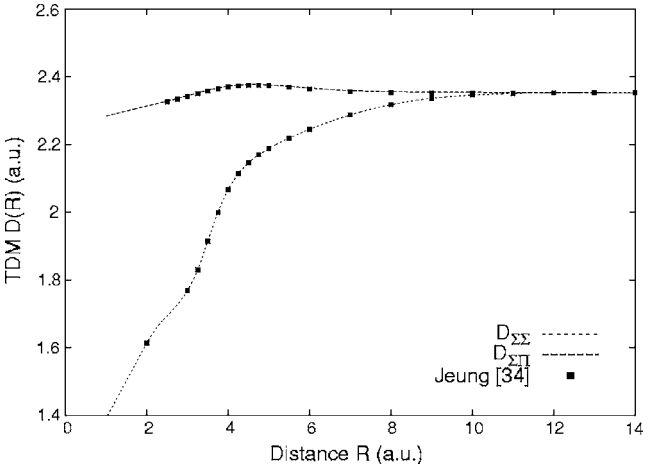

FIG. 3. The transition dipole moments $D(R)$ for the $\Sigma\Sigma$ and $\Sigma\Pi$ transitions against the internuclear separation R.

$$\tau=\frac{1}{A(v'J'\Lambda')}, \tag{10}$$

where

$$A(v'J'\Lambda')=\int_0^\infty d\epsilon'' A(v'J'\Lambda';\epsilon''J'\Lambda'') \tag{11}$$

is the total spontaneous emission rate corresponding to the transition from the upper bound level $(v'J'\Lambda')$ of the excited state $A\,^2\Pi$ to the lower continuum state $(\epsilon''J'\Lambda'')$ of the ground state $X\,^2\Sigma^+$ and

$$A(v'J'\Lambda';\epsilon''J'\Lambda'')=\frac{64\pi^4\nu^3}{3hc^3}g|\langle\phi_{v'J'\Lambda'}|D(R)|\phi_{\epsilon''J'\Lambda''}\rangle|^2 \tag{12}$$

is the probability of the spontaneous emission, with

$$g=\frac{2-\delta_{0,\Lambda'+\Lambda''}}{2-\delta_{0,\Lambda'}} \tag{13}$$

being the electronic degeneracy.

We assembled the results of our calculated lifetimes in Table IV. The high vibrational levels should be close to the radiative lifetime of the resonance state of the $2s$-$2p$ lithium atom. Our value 29.07 ns agrees quite well with the recent high-precision measured value 27.11 ns of Volz and Schmoranzer [37]. Carlsson and Sturesson [38] and McAlexander *et al.* [39] have measured, by using laser spectroscopy and pre-

TABLE IV. Lifetime τ (in ns) of the rovibrational levels of the $A\,^2\Pi$ state.

	$v=0$	$v=1$	$v=2$	$v=3$	$v=4$	$v=5$
$J=0$	61.61	53.24	45.21	38.42	32.94	29.07
$J=10$	59.59	50.93	42.76	35.59	29.34	
$J=20$	52.96	41.94				
$J=21$	51.89					

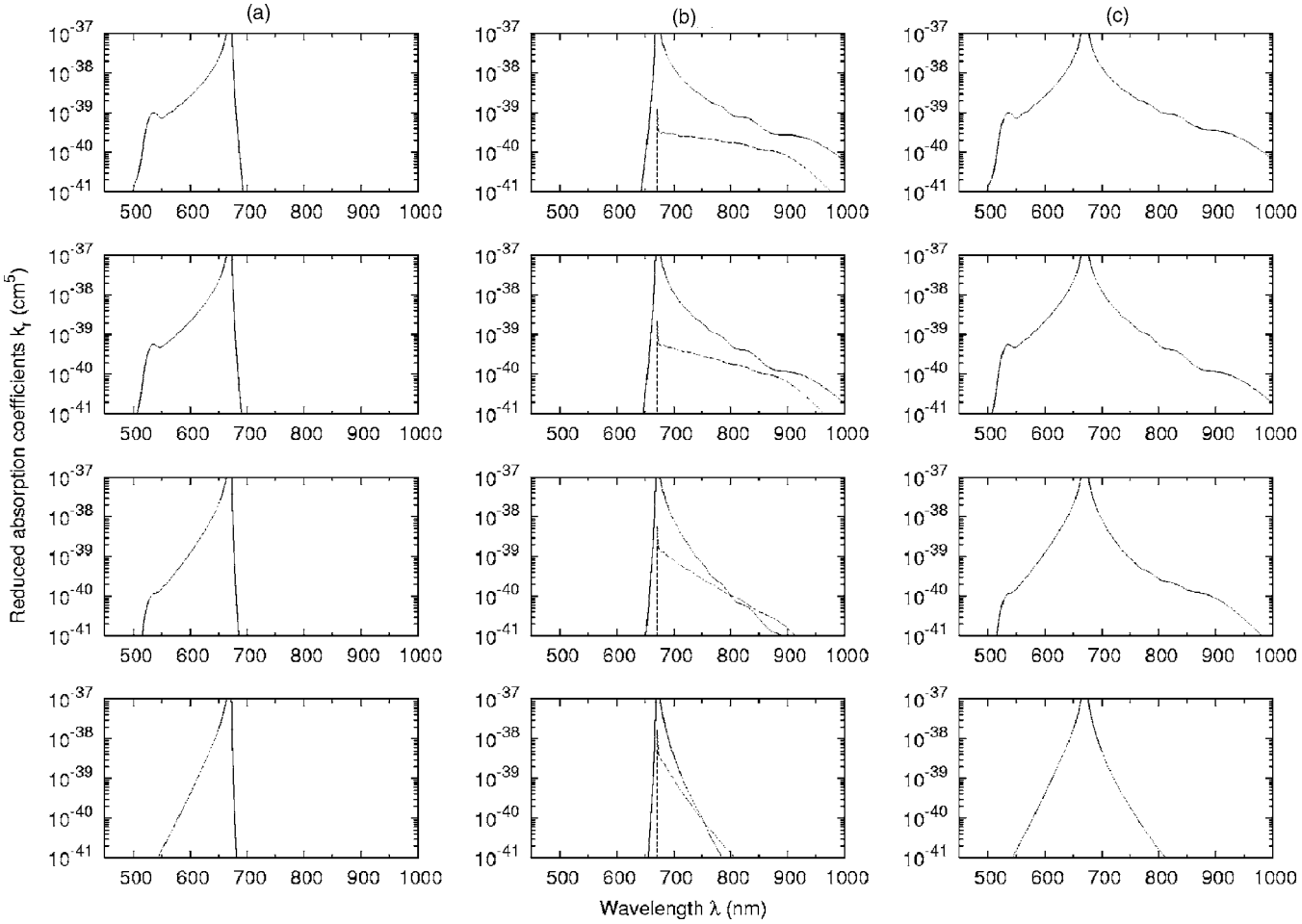

FIG. 4. Contributions to the reduced-absorption coefficient at the temperatures 500, 1000, 2000, and 3000 K presented, respectively, from the bottom to the top. Column (a) represents the free-free $X\,^2\Sigma^+$-$B\,^2\Sigma^+$ transitions and column (b) represents the free-free (solid line) and free-bound (dashed line) $X\,^2\Sigma^+$-$A\,^2\Pi$ transitions. Column (c) represents the sum of all the contributions.

dissociation analysis, 27.22 and 26.99 ns, respectively. All these experimental data do not differ more than 7.8% from our calculated lifetime value.

VI. RESULTS

A. Computational details

The Numerov method is used to solve numerically the radial-wave equation (8) and, particularly, to determine the normalized wave functions needed in the computation of the above matrix elements shown in Eqs. (5) and (7). We used the Gauss-Laguerre quadrature [40] with 100 weighted points to evaluate the free-free integral appearing in Eq. (5). One may notice that this integral diverges at large distances R. To circumvent this numerical problem, we have adopted the mathematical transformation outlined by Herman and Sando [15,41] and Dalgarno [30]

$$\langle \phi_{\epsilon' J' \Lambda'} | D(R) | \phi_{\epsilon'' J'' \Lambda''} \rangle = \langle \phi_{\epsilon' J' \Lambda'} | [D(R) - D_0] | \phi_{\epsilon'' J'' \Lambda''} \rangle + D_0 \frac{\langle \phi_{\epsilon' J' \Lambda'} | \Delta V(R) | \phi_{\epsilon'' J'' \Lambda''} \rangle}{\epsilon'' - \epsilon'}, \tag{14}$$

where $D(R)$ behaves asymptotically like $D(R) \sim D_0$.

Moreover, the reduced-absorption coefficients are carried out for different temperatures using the above Eqs. (5) and (7) with the frequency bin size $\Delta\nu = 10\ \mathrm{cm}^{-1}$. All the bound and quasibound levels are included in the calculations. Our simulations have particularly shown that the rotational quantum number J up to $J_{\max} = 26$ for the fb transitions and $J_{\max} = 250$ for the ff transitions are enough to accurately output the needed line shape for all the temperatures.

B. Reduced-absorption coefficient

The reduced-absorption coefficients in the far wings around the core resonance line $\lambda_0 = 670.8$ nm are determined by the transitions from the ground to the excited LiHe molecular states. The potential curves illustrated in Fig. 1 show that $X\,^2\Sigma^+$ and $B\,^2\Sigma^+$ electronic states are dominantly repulsive, whereas the $A\,^2\Pi$ state presents a shallow well. We may therefore consider only the absorption radiations resulting from the free-free X-A and X-B and free-bound X-A transitions. In all cases, the shape of the LiHe spectra consists of a blue wing due essentially to the X-B transitions and a red wing due to the X-A ones.

The full quantum-theoretical spectra in the range 450–1000 nm of the wavelength λ are presented in Fig. 4

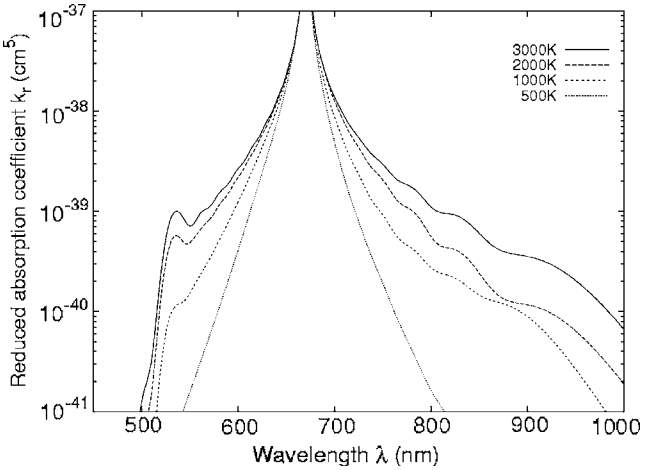

FIG. 5. Representation of the full quantum-mechanical reduced-absorption coefficients for different temperatures against the wavelength.

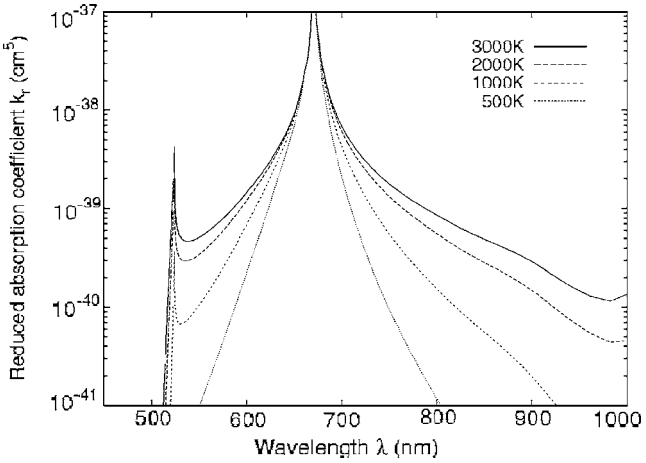

FIG. 6. The semiclassical reduced-absorption coefficients at four temperatures.

for four temperatures, $T=500$, 1000, 2000, and 3000 K. Columns (a) and (b) of this figure represent the partial contributions to the total spectra presented in column (c). Column (a) shows the *ff* contribution relative to the *X*-*B* transitions. As it can easily be seen, they are the main component in the blue wing and increase in magnitude as the temperature increases. It also shows the appearance of a satellite above approximately 1000 K. Column (b) presents the *ff* and *fb* contributions arising from the *X*-*A* transitions. In this case, both contributions contribute with almost the same intensity especially at the lower temperatures. The far red-wing spectra exhibit some undulations, which we believe are due to the quantum effects, i.e., the bound and mainly the quasibound levels. The sum of the three contributions is displayed in column (c) of Fig. 4. We also reproduce the same spectra in Fig. 5, which shows the effect of temperature on the total reduced-absorption coefficient. It particularly shows the occurrence of a satellite in the blue wing around 536 nm, which is in total accordance with the expected value found earlier from the potential difference. The satellite begins its appearance beyond $T \approx 1000$ K and its peak intensity grows with the temperature. One should point out that the second expected satellite around 1012 nm could not be reproduced in the far red wing by our quantal calculations. We think that the reasons for this failure may have been caused by the lack of accuracy in our constructed $A\ ^2\Pi$ potential curve, mainly in its short-range region, and/or transition dipole moment $D_{\Sigma\Pi}(R)$. We have also performed the classical calculations of the reduced-absorption coefficient at the same temperatures. Our results are plotted in Fig. 6. The shape of the spectra is generally found, though the undulations in the far wings are absent. On the other side, the classical calculations could yield the satellite structure in the blue wings. The peak is indeed observed for all temperatures at approximately the previous position, more precisely 524 nm.

To our knowledge, no experimental data of the absorption spectra are available in literature for comparison. However, very recent theoretical calculations have been carried out in almost the same range of temperatures [4,9]. In their full quantum-mechanical treatment of the LiHe emission spectra, Zhu, Babb, and Dalgarno [9] have nevertheless surveyed the absorption broadening. Their calculations, performed for temperatures between 200 and 3000 K, could determine a satellite at the position 536 nm in the blue wing. Besides, Allard *et al.* [4] have, within the frame of the unified theory, dealt theoretically with the absorption LiHe profile. The authors have particularly noted from their calculations the presence of a satellite structure in the far blue wing at about 500 nm. Furthermore, in both Refs. [4,9], the authors report the experimental work of Lalos and Hammond [42] on the emission spectra of hot dense gases in which they measured a satellite peak at the position 530 nm. A comparison of the line profile produced by our quantum-mechanical and classical calculations and by Allard *et al.* [4] is presented for $T=3000$ K in Fig. 7. The data provided to us by Allard [43] have been scaled so that they fit our spectra. The similarity of the general shape is demonstrated as well as the position of the satellite peaks.

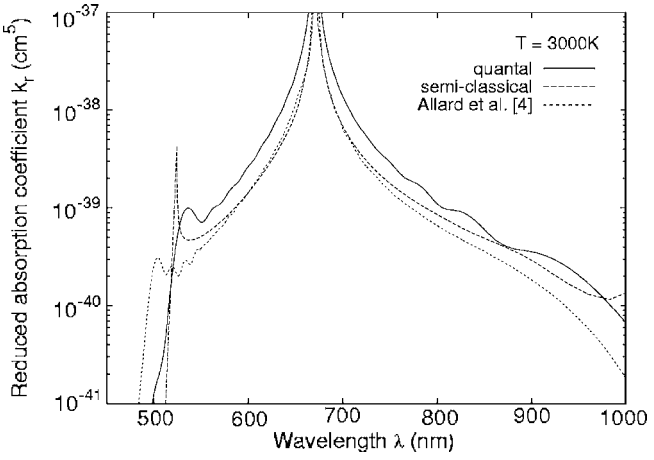

FIG. 7. Comparison between the results of the reduced-absorption coefficients at the temperature $T=3000$ K obtained quantum mechanically and classically. Both results are also compared with those obtained within the unified theory by Allard *et al.* [4].

VII. CONCLUSION

In this work, we have carried out at different temperatures quantum-mechanical and classical calculations of the reduced-absorption coefficients of the lithium resonance line Li($2s$-$2p$) when the radiating atoms are evolving in a ground helium gas. We have particularly constructed the ground and excited LiHe potential curves and the transition dipole moments that connect them. Our calculations could yield the satellite structure of the line profile and show the appearance of a satellite at the position close to 536 nm in the blue wing above $T \sim 1000$ K. Our results are compared with those deduced from the application of the unified theory. The agreement between all the results is generally found.

ACKNOWLEDGMENTS

A part of this work has been supported by the NSF through a grant for ITAMP, Smithsonian Center for Astrophysics, and Harvard Observatory. One of the authors (M.B.) is very grateful to Professor Alex Dalgarno for his support while in Harvard Observatory and for providing him with some needed data. The authors would also like to thank Dr. N. Allard for providing the LiHe profile data.

[1] J. F. Babb, K. Kirby, and H.-K. Chung, in *Proceedings of the NASA Laboratory Astrophysics Workshop*, edited by F. Salama (Ames Research Center, 2002).
[2] S. L. Hawley, in *Proceedings of the 12th Cambridge Workshop on Cool Stars, Stellar Systems, and the Sun*, edited by A. Brown, G. M. Harper, and T. R. Ayres (University of Colorado, 2003).
[3] N. F. Allard, F. Allard, P. H. Hanschildt, J. F. Kielkopf, and L. Machin, A & A **411**, L473 (2003).
[4] N. F. Allard, F. Allard, and J. F. Kielkopf, A & A **440**, 1195 (2005).
[5] C. Vadla, R. Beuc, V. Horvatic, M. Movre, A. Quentmeier, and K. Niemax, Eur. Phys. J. D **37**, 37 (2006).
[6] H.-K. Chung, K. Kirby, and J. F. Babb, Phys. Rev. A **60**, 2002 (1999).
[7] H.-K. Chung, K. Kirby, and J. F. Babb, Phys. Rev. A **63**, 032516 (2001).
[8] H.-K. Chung, M. Shurgalin, and J. F. Babb, AIP Conf. Proc. No. 645 (AIP, New York, 2002).
[9] C. Zhu, J. F. Babb, and A. Dalgarno, Phys. Rev. A **71**, 052710 (2005).
[10] C. Zhu, J. F. Babb, and A. Dalgarno, Phys. Rev. A **73**, 012506 (2006).
[11] R. O. Doyle, J. Quant. Spectrosc. Radiat. Transf. **8**, 1555 (1968).
[12] K. M. Sando and A. Dalgarno, Mol. Phys. **20**, 103 (1971).
[13] C. Bottcher, A. Dalgarno, and E. L. Wright, Phys. Rev. A **7**, 1606 (1973).
[14] R. Scheps, Ch. Ottinger, G. York, and A. Gallagher, J. Chem. Phys. **63**, 2581 (1975).
[15] P. S. Herman and K. M. Sando, J. Chem. Phys. **68**, 1153 (1978).
[16] W. Behmenburg *et al.*, J. Phys. B **29**, 3891 (1996).
[17] T. Grycuk, W. Behmenburg, and V. Staemmler, J. Phys. B **34**, 245 (2001).
[18] W. Behmenburg *et al.*, J. Phys. B **35**, 747 (2002).
[19] J. Szudy and W. E. Baylis, J. Quant. Spectrosc. Radiat. Transf. **15**, 641 (1975).
[20] N. F. Allard and J.F. Kielkopf, Rev. Mod. Phys. **54**, 1103 (1982).
[21] J. Szudy and W. E. Baylis, Phys. Rep. **266**, 127 (1996).
[22] E. Czuchaj, F. Rebentrost, H. Stoll, and H. Preuss, Chem. Phys. **196**, 37 (1995).
[23] V. Staemmler, Z. Phys. D: At., Mol. Clusters **39**, 121 (1997).
[24] G.-H. Jeung (private communication, 2000).
[25] C. J. Lee, M. D. Havey, and R. P. Meyer, Phys. Rev. A **43**, 77 (1991).
[26] A. Nakayama and K. Yamashita, J. Chem. Phys. **114**, 780 (2001).
[27] M. Krauss, P. Maldonado, and A. C. Wahl, J. Chem. Phys. **60**, 4944 (1971).
[28] M. Jungen and V. Staemmler, J. Phys. B **21**, 463 (1988).
[29] Z. C. Yan, J. F. Babb, A. Dalgarno, and G. W. F. Drake, Phys. Rev. A **54**, 2824 (1996).
[30] A. Dalgarno (private communication).
[31] J.-M. Zhu, B.-L. Zhou, and Z. C. Yan, J. Phys. B **34**, 1535 (2001).
[32] R. J. Le Roy, FORTRAN, Level 7.4 program, University of Waterloo, Chemical Physics Research Report (2001).
[33] G. F. Gribakin and V. V. Flambaum, Phys. Rev. A **48**, 546 (1993).
[34] G.-H. Jeung (private communication, 2001).
[35] J. Pascale, Phys. Rev. A **28**, 632 (1983).
[36] X. Chu and A. Dalgarno, Phys. Rev. A **66**, 024701 (2002).
[37] U. Volz and H. Schmoranzer, Phys. Scr., T **65**, 48 (1996).
[38] J. Carlsson and L. Sturesson, Z. Phys. D: At., Mol. Clusters **14**, 281 (1989).
[39] W. L. McAlexander *et al.*, Phys. Rev. A **51**, R871 (1995).
[40] W. H. Press, B. P. Flannery, S. A. Teukolsky, and W. T. Vetterling, *Numerical Recipes: The Art of Scientific Computing* (Cambridge University Press, New York, 1987).
[41] K. M. Sando and P. S. Herman, in *Spectral Line Shapes*, edited by K. Burnett (Walter de Gruyter & Co, Berlin, 1983).
[42] G. T. Lalos and G. L. Hammond, Astrophys. J. **135**, 616 (1962).
[43] N. F. Allard (private communication).